Journal of Earth Science, *Vol. 25*, *No. 2*, *p. 357–365*, *April 2014* *ISSN 1674-487X*
Printed in China
DOI: 10.1007/s12583-014-0416-8

Understanding Miocene Climate Evolution in Northeastern Tibet: Stable Carbon and Oxygen Isotope Records from the Western Tianshui Basin, China

Zhanfang Hou*[1, 2, 3, 4], Jijun Li[2, 3, 5], Chunhui Song[3, 6], Jun Zhang[2, 3], Zhengchuang Hui[2, 3], Shiyue Chen[7], Feng Xian[1]

1. *State Key Laboratory of Loess and Quaternary Geology*, *Institute of Earth Environment*, *Chinese Academy of Sciences*, *Xi'an* 710054, *China*
2. *College of Earth and Environmental Sciences*, *Lanzhou University*, *Lanzhou* 730000, *China*
3. *MOE Key Laboratory of Western China's Environmental Systems*, *Lanzhou University*, *Lanzhou* 730000, *China*
4. *Graduate University of Chinese Academy of Sciences*, *Beijing* 100039, *China*
5. *College of Geography Sciences*, *Nanjing Normal University*, *Nanjing* 210097, *China*
6. *School of Earth Sciences*, *Lanzhou University*, *Lanzhou* 730000, *China*
7. *College of Environment and Planning*, *Liaocheng University*, *Liaocheng* 252000, *China*

ABSTRACT: To investigate climate evolution during the Miocene, especially during the Middle Miocene climate transition on the northeastern Tibetan Plateau, stable oxygen and carbon isotopes of carbonates from a 288-m-thick lacustrine-fluvial sediment sequence covering the period from 17.1 to 6.1 Ma from Tianshui Basin, China, were analyzed. The relatively low stable oxygen isotope values indicate the prevalence of wet climate conditions during the period of 17.1–13.6 Ma, an interval corresponding to the well-known Middle Miocene Climate Optimum. The interval between 13.6 and 11.0 Ma (i.e., the late Middle Miocene) is marked by a progressive increase in the $\delta^{18}O$ values, indicative of a decrease in precipitation, probably linked to the expansion of the East Antarctic Ice Sheet and global cooling since about 14 Ma. The climate in the study area continued to get drier as shown by the enrichment of the heavy oxygen isotope from 11 Ma. We attribute these stepwise climatic changes as revealed by our carbonate $\delta^{18}O$ record from the northeastern Tibetan Plateau to the sustained global cooling that may have reduced moist transport to Central Asia, which in turn led to a permanent aridification.
KEY WORDS: stable oxygen, carbon isotope, climate change, Miocene, Tianshui Basin.

1 INTRODUCTION

There has been an increasing consensus that the Miocene is a period of progressive climatic deterioration, during which the Earth's climate system underwent a remarkable cooling associated with the expansion of the East Antarctic Ice Sheet (EAIS) (Zachos et al., 2001; Miller et al., 1987; Shackleton and Kennett, 1975). Specifically, global climate was warm during the Early to Middle Miocene, which is usually referred as the Middle Miocene Climatic Optimum (MMCO). Climate began to get cool from the late Middle Miocene associated with the expansion of the EAIS (Zachos et al., 2001; Miller et al., 1987; Shackleton and Kennett, 1975). Mg/Ca record from benthic foraminifera shows a similar cooling trend (Lear et al., 2000). During the late Middle Miocene, temperatures in middle and high latitudes dropped sharply associated with the expansion of the EAIS, while temperatures in low latitudes remained stable and even rose slightly in some areas (Flower and Kennett, 1994; Savin et al., 1975), thereby enlarging the meridional temperature gradient and extending the width of the climatic zones; together, leading to the aridity in the middle- and high-latitude continental interiors such as Australia (Robert et al., 1986; Stein and Robert, 1986), Africa (Retallack, 1992), North America (Webb, 1997; Wolfe, 1985), and South America (Pascual and Janreuizar, 1990). There are only few continental records during the Miocene from the Asia interior (Jiang and Ding, 2010, 2008; Jiang et al., 2008; Chung and Koh, 2005; Wang et al., 2001). Moreover, the mechanism of aridification in inland Asia, the largest mid-latitude arid zone in the Northern Hemisphere, still remains controversial. Numerical modeling reveals that the uplift of the Tibetan Plateau and the retreat of the Paratethys Sea may have played significant roles in the initiation and development of the arid zone in Asia's interior (Zhuang et al., 2011; An et al., 2001; Ramsein et al., 1997), while other studies indicate that global cooling was the culprit (Hui et al., 2011; Jiang and Ding, 2010; Lu et al., 2010; Jiang and Ding, 2008; Jiang et al., 2008; Guo et al., 2004).

Based on the onset of eolian deposition, it was argued that an enhanced aridification in Asia's interior may have occurred after 8 Ma (An et al., 2001). Recently, a study from the

*Corresponding author: houzf@ieecas.cn

Manuscript received September 21, 2012.
Manuscript accepted January 27, 2013.

Hou, Z. F., Li, J. J., Song, C. H., et al., 2014. Understanding Miocene Climate Evolution in Northeastern Tibet: Stable Carbon and Oxygen Isotope Records from the Western Tianshui Basin, China. *Journal of Earth Science*, 25(2): 357–365, doi:10.1007/s12583-014-0416-8

Tianshui Basin, northeast of the Tibetan Plateau suggests that the aridification might have initiated as early as from 22 Ma, based on field observation, mineral assemblage, grain size and morphology of fine-grained Neogene sediments, which is similar to that of Quaternary loess (Guo et al., 2002). This timing is about 14 Ma earlier than previously thought. However, a few isotopic studies from Nepal and the northeastern Tibetan Plateau suggests that the aridification in the interior Asia may have begun at 13–11 Ma (Hough et al., 2011; Zhuang et al., 2011; Dettman et al., 2003, 2001).

In northern China, there are numerous Cenozoic sedimentary basins where thick fluvial-lacustrine deposits may provide us with important information on the long-term climate history of interior Asia (Hui et al., 2011; Jiang and Ding, 2008; Jiang et al., 2008, 2007; Wang and Deng, 2005; Fang et al., 2003; Li and Ku, 1997). In this study, the $\delta^{13}C$ and $\delta^{18}O$ of carbonates from a well-exposed section that is magnetically dated (Zhang et al., 2013) in the Tianshui Basin, northeastern Tibetan Plateau, were analyzed to explore the aridification history of the interior Asia during the Miocene. By comparing with other records in adjacent areas, we discussed the pattern of regional climate changes in the Asian Interior within the context of global climate changes during the Miocene.

2 ECOLOGICAL AND GEOGRAPHICAL SETTING

The Tianshui Basin is located at the northeastern margin of the Tibetan Plateau (Fig. 1a). It is a tectonic graben bordered to the north by the left-lateral strike-slip Haiyuan fault, to the east and northeast by the Liupan Shan, and to the south by the western Qinling Mountain (Fig. 1b). The basin is situated in the intersection of the East Asian monsoon area, the northwest arid area, and the Tibet Plateau cold and arid regions, where climate is very sensitive to the changes in the atmospheric circulation pattern. Continuous and widespread mudflat/distal fan as well as Neogene shallow lake deposits distributed in this basin provide an ideal setting for studying the paleoclimate history of western China (Zhang et al., 2013; Hui et al., 2011; Alonso-Zarza et al., 2009; Li et al., 2006).

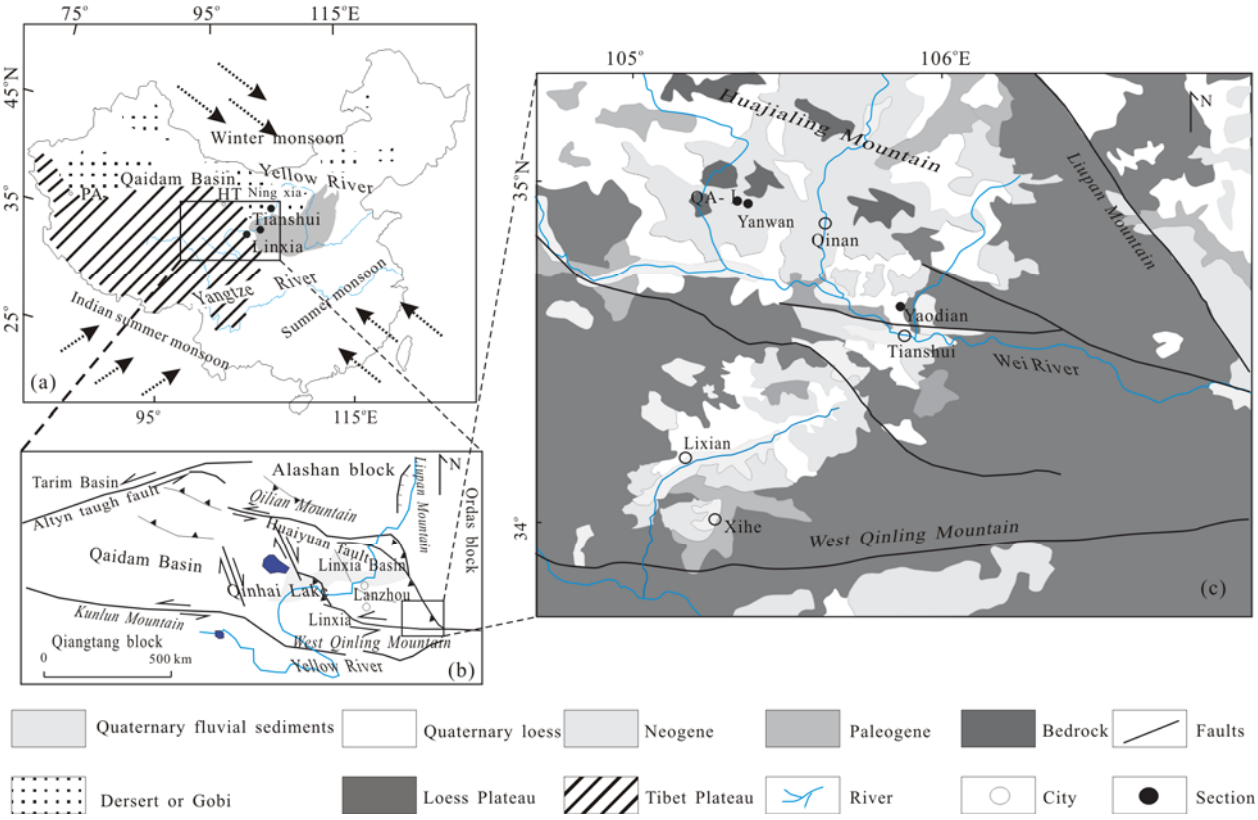

Figure 1. Map showing the location of the Tianshui Basin, China and the Yanwan Section (redrawn from Alonso-Zarza et al., 2009).

The Yanwan (YW) Section (34º58′N, 105º34′E) lies about 14 km northwest of Qin'an County, Gansu Province (Fig. 1c). Overlying unconformably the metamorphic rocks of the Sinian Formation, the Neogene sequence consists of about 288 m thick lacustrine-fluvial sediments, which is capped by about 60 m thick Quaternary loess. Three lithostratigraphic units can be distinguished according to the lithologic properties and depositional characteristics (Zhang et al., 2013). The basal unit (Unit I) is 132 m thick, and it is characterized by fine-grained light brownish-yellowish mudstones intercalated with brownish-reddish mudstone deposited in a floodplain environment; the middle unit (Unit II) is about 128 m thick, which consists mainly light brownish-yellowish calcareous mudstones interbedded with brownish-reddish mudstones with fine laminations corresponding to a lacustrine mudflat with sheet-floods environment. This unit is also characterized by two fossiliferous layers containing abundant Hipparion fauna fossils (Fig. 2); the upper unit (Unit III) is 28 m think, which is mainly composed

of brownish-reddish and brownish-yellowish mudstones with horizontal bedding and grayish-greenish bands, corresponding to a floodplain/distal fan environment (Zhang et al., 2013; Alonso-Zarza et al., 2009; Li et al., 2006). The YW Section is well dated based on fossil mammal assemblages and paleomagnetic polarity studies (Fig. 2; Zhang et al., 2013).

3 METHODS

A total of 135 samples of mudstone/muddy siltstone, marls, calcium nudules, and mixed marls were collected at ca. 2.1 m intervals (equivalent to a temporal resolution of 80 ka). The $\delta^{13}C$ and $\delta^{18}O$ of the pedogenic and lacustrine carbonate in the samples were measured using an automated carbonate preparation device (KIEL-III) coupled to a Finnigan MAT 252 isotope ratio mass spectrometer. CO_2 gas liberated from the carbonate was extracted by reacting ground samples of 20–300 μg with dehydrated phosphoric acid in a vacuum at 70 ℃. The results are presented using the delta notation referred to the VPDB standard. Repeated measurements (n=6) of a homogenized sample yields a standard deviation of ±0.1‰ and ±0.06‰ for $\delta^{18}O$ and $\delta^{13}C$ measurements, respectively. Seven selected lacustrine samples were powdered for X-ray diffraction analysis, which was performed with a Bruker D8 Advance Diffractometer using Cu Kα radiation. Carbonate mineralogy was determined based on the position of the d (104) peak.

4 RESULTS

The stable carbon and oxygen isotope records presented here cover the time interval of 17.1–6.1 Ma (Fig. 2). The oxygen isotope values vary from -7.5‰ to -12.5‰, with a phased enrichment toward more positive values. Paleosol calcite nodules and flood mudstone from the lower YW Section (Phase I: 17.1–13.6 Ma) exhibit more negative $\delta^{18}O$ values ranging from -12.5‰ to -9.5‰ with an average of ca. -10.8‰ (n=42). The $\delta^{18}O$ values increased to -10‰ between 13.6 and 11 Ma (Phase II) (n=25). There is a more prominent positive shift in $\delta^{18}O$ values to -9.1‰ (n=68) around 11 Ma, and relatively high values were maintained until 7.1 Ma. The shift in $\delta^{18}O$ values from Phase I to Phase III is 1.7‰. The average of $\delta^{13}C$ values during phases I, II, and III is -7.1‰, -7.4‰, and -8.3‰, respectively.

Li et al. (2013) proposed that the primary (endogenous) carbonate has high Mn/Ca and Mg/Ca ratios, while secondary (exogenous) carbonate has low Mn/Ca and Mg/Ca ratios. In the Yanwan Section, XRD analysis (Fig. 3) on three typical lacustrine carbonate samples shows that low-Mg calcite (LMC) is the dominant carbonate mineral (Goldsmith et al., 1955). Our results are consistent with mineralogical studies on the Tibetan

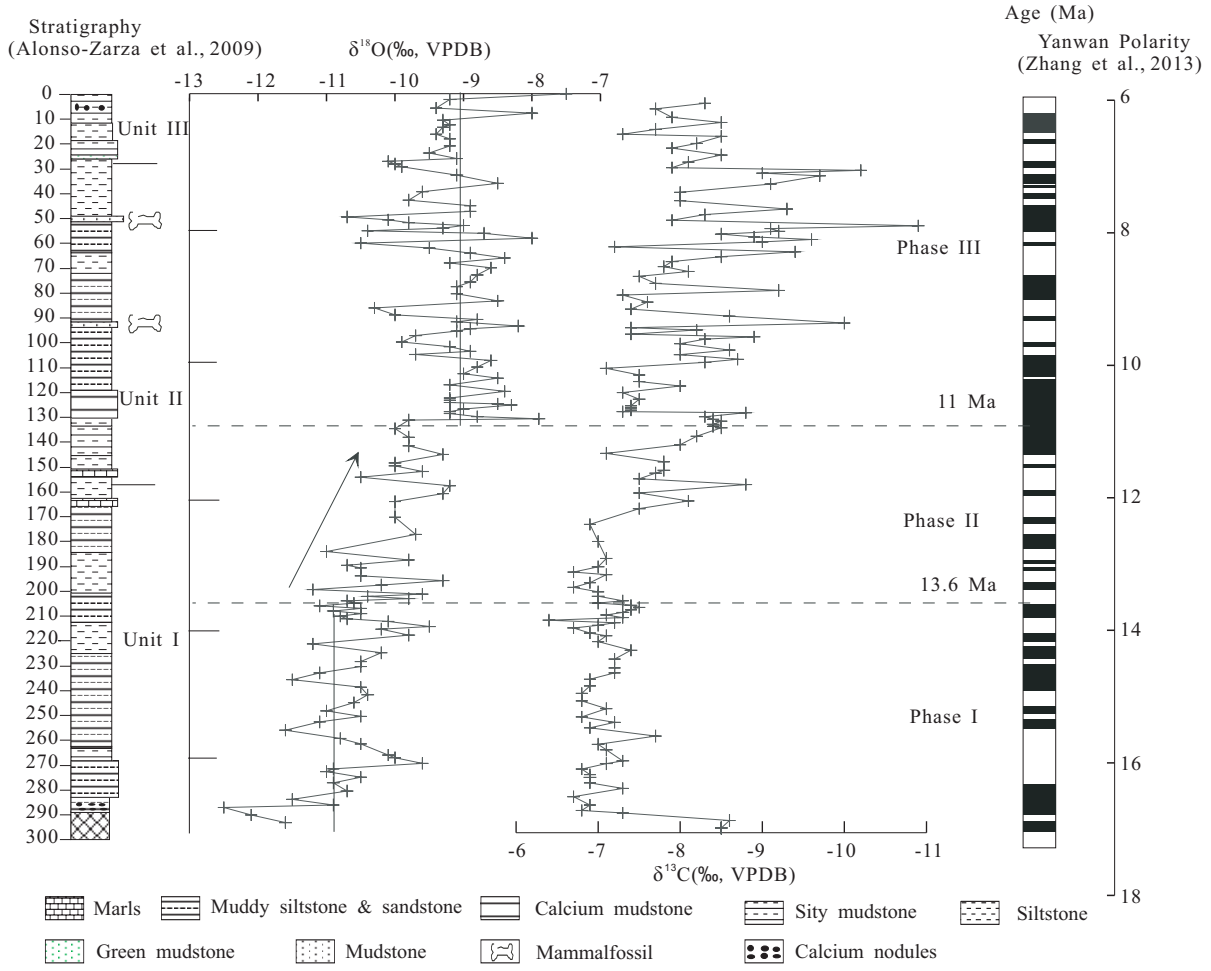

Figure 2. $\delta^{18}O$ and $\delta^{13}C$ records from the Yanwan Section, Tianshui Basin, China. Age assignments of measured samples are linearly interpolated based on magnetostratigraphy and biostratigraphy (Zhang et al., 2013).

Plateau (Zhuang et al., 2011; Fan et al., 2007; Cyr et al., 2005). The mineral composition implies that our samples might have been composed of certain proportions of detrital carbonates. While distinguishing authigenic carbonate from detrital carbonate is of great importance for deciphering the climatic history beared in our $\delta^{13}C$ and $\delta^{18}O$ records, we argue that if detrital carbonates were present in our samples, they may represent a baseline signal over which the $\delta^{13}C$ and $\delta^{18}O$ varied through time at the Yanwan Section, given a stable sediment supply from the South Qinling Mt. and North Huajialing Mt. (Alonso-Zarza et al., 2009). Therefore, the $\delta^{13}C$ and $\delta^{18}O$ values of the bulk samples can be used for paleo-environmental studies.

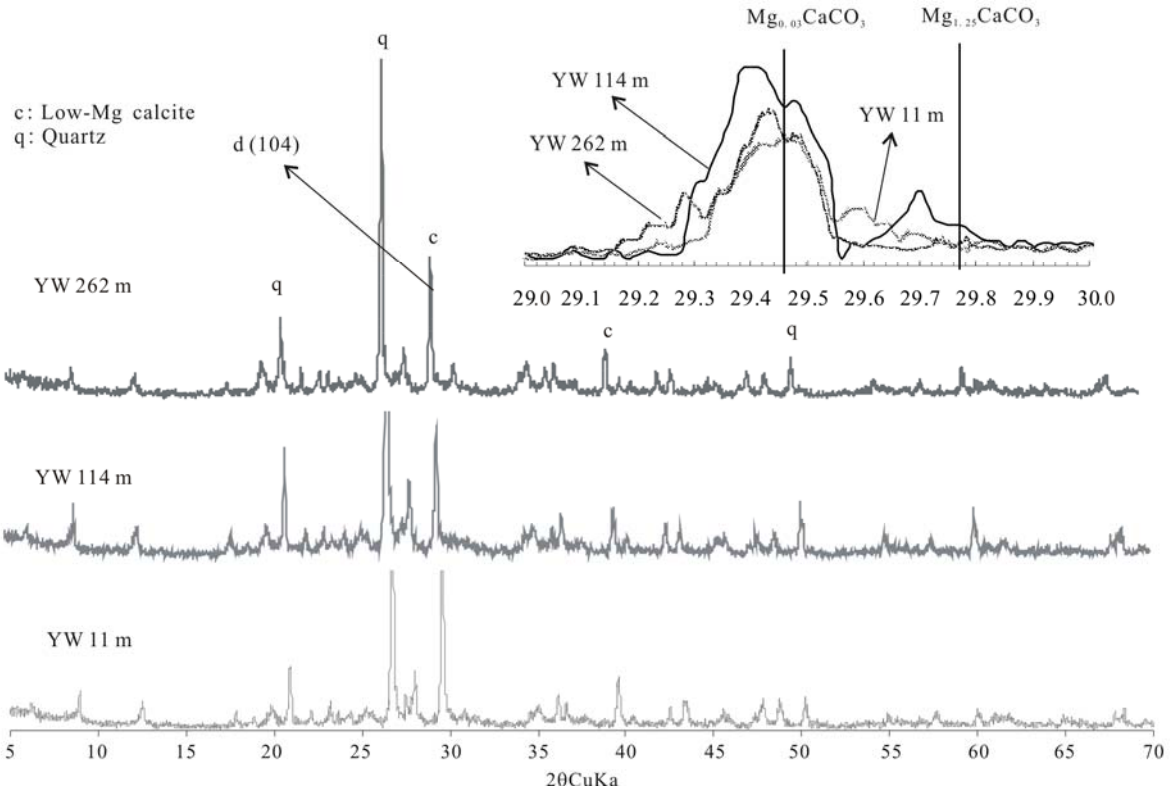

Figure 3. XRD patterns of representative samples in Tianshui Basin. Note that the positions of d (104) peak correspond to low Mg calcite. The two solid lines indicate the d (104) peak of pure low-Mg calcite ($Mg_{0.03}CaCO_3$) and pure high-Mg calcite ($Mg_{1.25}CaCO_3$) (www.icdd.com, PDF 2004).

5 DISCUSSION

In closed lake systems, intensified evaporation and/or prolonged residence time of the lake water may cause the enrichment of the heavy oxygen isotope in lake waters, while enhanced biologic production and equilibration with atmospheric CO_2 exchange associated with prolonged water residence time would increase the $\delta^{13}C$ values of dissolved inorganic carbon (Leng and Marshall, 2004). A high correlation (R^2>0.7) between $\delta^{18}O$ and $\delta^{13}C$ values was widely used as a paleohydrological indicator for closed lake system (Li and Ku, 1997; Talbot, 1990). However, the $\delta^{18}O$ and $\delta^{13}C$ values of our samples (n=135) show a poor correlation (Fig. 4), suggesting an open lake system as observed in other lakes on the Tibetan Plateau (Cyr et al., 2005; Talbot, 1990). Therefore, the evaporative effects may have contributed little to the observed positive shift in oxygen isotope values in this open lake system.

The $\delta^{18}O$ values of carbonates are controlled by both the $\delta^{18}O$ composition and temperature of surface waters. For an open lake system, the $\delta^{18}O$ composition of lake water is mainly controlled by that of meteoric precipitation. In lake systems, micritic carbonates typically precipitate in the late spring and early summer, as the water warms up and the saturation of the lake water increases (Goldsmith et al., 1961). Therefore, the authigenic carbonates may precipitate in a relatively narrow range of temperature. It is also noted, however, that the $\delta^{18}O$ values of carbonate are not strongly affected by temperature. A

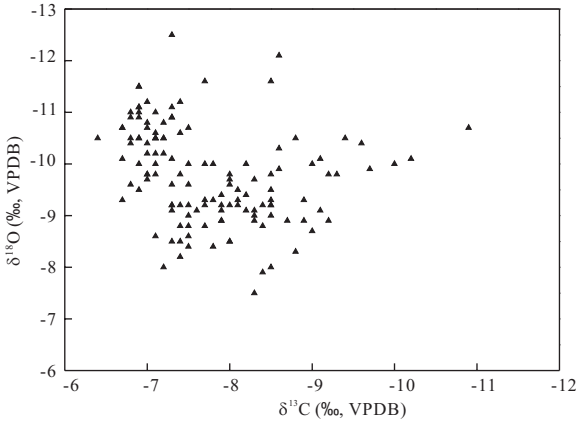

Figure 4. Biplot of $\delta^{13}C$ versus $\delta^{18}O$ values of the YW Section. The lack of correlation suggests a hydrologically open lake system.

change in temperature of 4.3 ℃ can lead to a very small change (~1‰) in the $\delta^{18}O$ values of carbonate (Kim and O'Neil, 1997). A cooling of about 7 ℃ would lead to carbonates that are 1.7‰ more positive from Phase I to III, but lower atmospheric temperatures tend to drive the $\delta^{18}O$ of precipitation toward more negative values (Rozanski et al., 1993). Thus, these two trends can come close to canceling each other out (Dettman et al., 2003). Therefore, the temperature effect may contribute little to the variation of the $\delta^{18}O$ in the Tianshui Basin.

Another possible factor contributing to this 1.7‰ shift may be the change in the $\delta^{18}O$ of the seawater, which is the ultimate source of meteoric water in the Tianshui Basin. Flower (1993) argued that the $\delta^{18}O$ of Pacific Ocean benthic foraminifera increased by approximately 1.2‰ (VPDB) during the Middle Miocene. They argued that the oxygen isotope ratios of both benthic and planktonic foraminifera increased by 0.3‰ in the Pacific Ocean, which is attributed to an increase in the $\delta^{18}O$ values of seawater between 13.2 and 13 Ma (Flower, 1993). However, the oxygen isotope record of the Yanwan Section shows no obviously change during this period. And they also suggested that a large shift of 0.7‰ in the $\delta^{18}O$ of sea-water occurred between 14.1 and 14.7 Ma (Flower, 1993), whereas this change clearly preceded the increase of $\delta^{18}O$ as seen in our record (Fig. 2). Therefore, if an increased in the $\delta^{18}O$ value of the seawater source occurred around 13.6 and 11.0 Ma, it would have only a small contribution to the 1.7‰ change and the oxygen isotopic change mainly reflects the variation of precipitation in the Tianshui Basin. Therefore, we conclude that the $\delta^{18}O$ values of lacustrine carbonate were mainly controlled by the $\delta^{18}O$ composition of the meteoric water. The more negative $\delta^{18}O$ values indicate higher amount of precipitation and a wetter climatic condition and vice versa.

The factors affecting the carbon isotopic signature of lacustrine deposits are very complicated. There are three primary controlling factors on the $\delta^{13}C$ values of lacustrine carbonates: (1) groundwater and riverine water discharge. Generally, groundwater and riverine water have low $\delta^{13}C_{TDIC}$ (total dissolved inorganic carbon) values. Therefore, higher fresh water inflow to a lake under wetter climatic conditions may lead to lower $\delta^{13}C$ values of carbonates. (2) Aquatic primary production. During periods of enhanced biological productivity, or in water systems with a large biomass, the ^{12}C is preferentially incorporated into the biomass, which in turn would lead to a relative enrichment of the ^{13}C in the lake water and thus the carbonate derived therein. (3) CO_2 exchange between the atmosphere and water. Under warm climatic conditions, the dissolved CO_2 in the lake water preferentially releases the ^{12}C, thereby resulting in more positive $\delta^{13}C$ values of the carbonates. Therefore, using carbon isotopic composition in the lacustrine carbonates to infer climate change tends to be difficult due to these complicated factors.

Based on oxygen isotopic composition of carbonates, we provide a long, continuous record of palaeoclimatic evolution in western China. Our record shows that regional climate experienced three major phases, albeit with some short-term fluctuations.

Phase I: Middle-Miocene (17.1–13.6 Ma). The minimum $\delta^{18}O$ value during this period indicates the highest precipitation. Sporopollen records as well as the discovery of Miocene assemblage of mammals (*Platybelodon* and *Acertherium*) in the same section also indicate a climate optimum during this period (Zhang et al., 2013; Hui et al., 2011). Based on oxygen isotope evidences and pollen data, this event is also apparent in the Qaidam Basin of the northern Tibetan Plateau (Zhuang et al., 2011; Miao et al., 2011; Kent-Corson et al., 2009). The $\delta^{18}O$ record, mammal assemblage, and plants fossil evidence from the Linxia Basin indicate very wet climate before about 13 Ma (Dettman et al., 2003; Ma et al., 1998; Zhai et al., 1959). In the Ningxia Basin, pollen records also reflect a modest climatic condition before about 14 Ma (Jiang and Ding, 2008; Jiang et al., 2008).

The climate optimum coincides well with the well-known MMCO registered in global deep-sea records (Zachos et al., 2008, 2001; Flower and Kennett, 1994) as well as in the record from the South China Sea (Cheng et al., 2004). The Middle Miocene climate optimum has been reported by many studies elsewhere, such as northern South China Sea (Wei et al., 2006; Clift et al., 2002), southeast coastal area of China (Zou et al., 2004), East Asia (Saito et al., 1995; Itoigawa and Yamanoi, 1990) and America (White et al., 1997).

Phase II: 13.6–11.0 Ma (204–137 m). The positive shift of the $\delta^{18}O$ values during this period indicates a decrease in precipitation. The sporopollen record of the same section also shows that the climatic condition was less humid than that before 14.7 Ma (Hui et al., 2011). This drying trend also appeared in neighboring regions. For example, in Linxia Basin, the oxygen isotope records indicate a decreasing trend of precipitation during 13–11 Ma (Wang and Deng, 2005; Dettman et al., 2003). In the Ningxia and Qaidam basins, pollen records and oxygen isotope evidence also reflect a significant decline in the East Asian summer monsoon, reflecting the same drying trend during the period (Miao et al., 2011; Zhuang et al., 2011; Kent-Corson et al., 2009; Jiang and Ding, 2008; Jiang et al., 2008, 2007).

The drying trend during this period is substantially synchronous with the well-known Middle-Miocene cooling (Fig. 5), which has been regarded as the result of a major expansion and semi-permanent establishment of the EAIS concurrent with deep water cooling (Holbourn et al., 2005; Singh and Gupta, 2005; Miller et al., 1996, 1991; Flower and Kennett, 1994). The expansion and semi-permanent establishment of the EAIS may have decreased temperatures in high latitudes, while low-latitude temperatures remained relatively constant, leading to a significant enlargement in the polar-equator temperature gradient (Savin et al., 1975). Such a change in the meridional temperature gradient brought increased aridity, especially in middle- to high-latitude continental regions (Retallack, 1992; Stein and Robert, 1986; Wolfe, 1985). Jiang and Ding, (2008) suggested that cooling and ice-sheet expansion over the polar region may have caused an increase in meridional temperature gradients, leading to a southward retreat of the monsoon circulation and thus a decreasing in precipitation in northern China. Therefore, we attribute the decline of the precipitation between 13.6 and 11.0 Ma to the Middle Miocene cooling and EAIS growth.

Phase III: 11.0–6.1 Ma (137–0 m). The prominent shift in $\delta^{18}O$ values toward more positive values reflects enhanced aridity. This climatic change has also been revealed by various proxies from previous studies in the adjacent regions. Pollen and other climatic proxies from Ningxia Basin show that

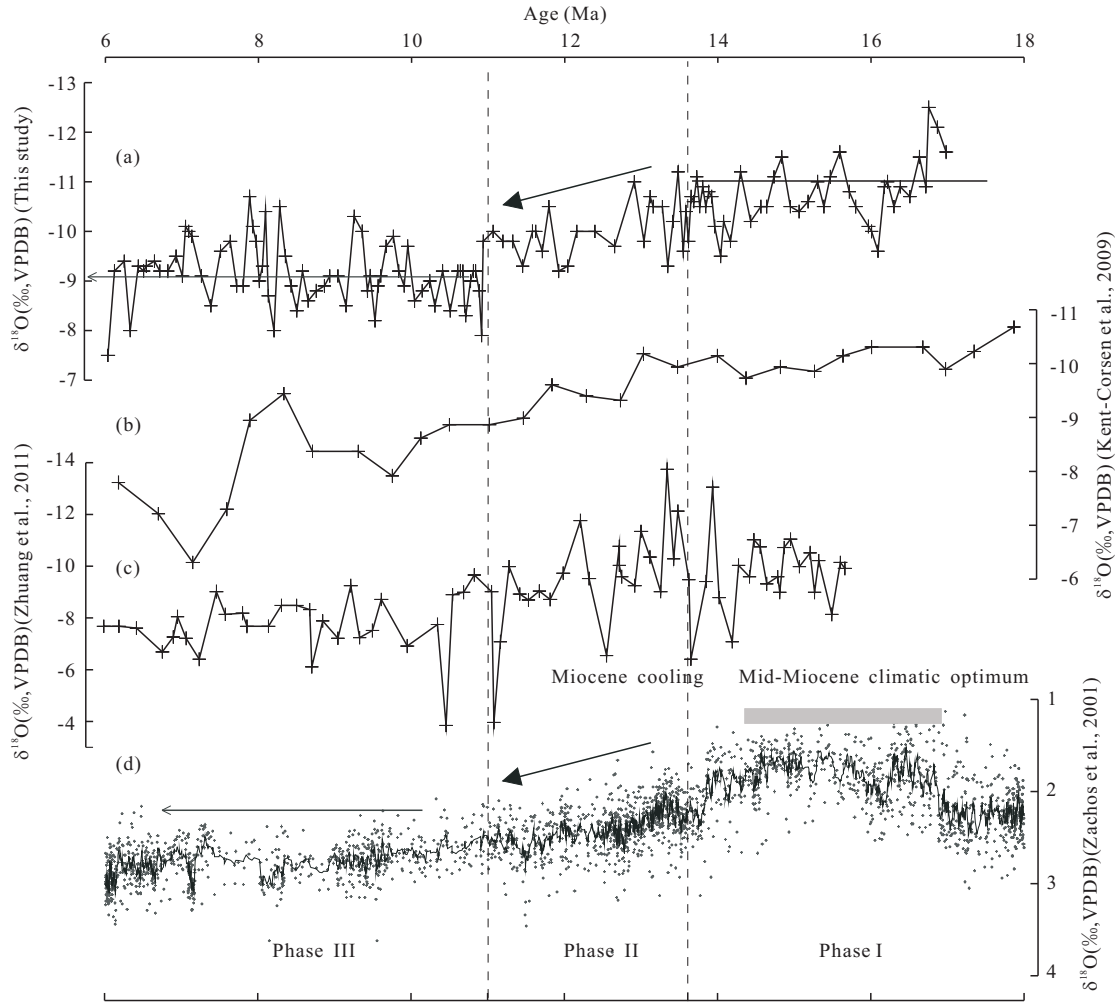

Figure 5. (a) Correlation of the $\delta^{18}O$ values from the Yanwan Section, Tianshui Basin, China; (b) the $\delta^{18}O$ values from Pianaman Section (Kent-Corson et al., 2009); (c) the $\delta^{18}O$ values from Huaitoutala Section (Zhuang et al., 2011); (d) the synthesized oxygen isotopes (7-point running average) from (Zachos et al., 2001).

climate became gradually drier since around 11.0 Ma (Jiang and Ding, 2008; Jiang et al., 2008). Both the thriving of Cypridis and oxygen isotope records from Qaidam Basin indicate a drying climate trend after 10.7 Ma (Zhuang et al., 2011; Kent-Corson et al., 2009; Yang et al., 2000; Fig. 5) as a manifestation of an intensified aridity in northern China around 11 Ma.

The development of the EAIS and the propagation of the global cooling signal occurred since 14 Ma (Zachos et al., 2001). Thus, it is difficult to explain the striking shift of the $\delta^{18}O$ values in Tianshui Basin since about 11 Ma. The uplift of the Tibetan Plateau $\delta^{18}O$ at about 12–11 Ma might have played a possible role (Zhuang et al., 2011; Dettman et al., 2003, 2001), although definitive evidence on the timing of the uplift remains fragmentary (Li G J et al., 2011; Guo et al., 2002; An et al., 2001; Li J J et al., 1997). The lithology of the YW Section is characterized by continuous mudstone without hiatuses. Therefore, the linkage between the uplift of the Tibetan Plateau and the aridification in Central Asia is far from conclusive because of the poor constraints on the timing and amplitude of the uplift; rather, a connection between global cooling and aridification in central Asia appears to be more convincing (Lu et al., 2010).

The supplies of water vapor from the subtropical and tropical oceans have significantly decreased during the development of the EAIS and the lowering of global sea level during the late Middle Miocene (Barron, 1985). According to John (2004), a 50±5.0 m lowering of global sea level occurred during the late Middle Miocene events (Mi3 and Mi4). It supports the notion that the volume of EAIS reached its peaks by 12–10 Ma (Shackleton and Kennett, 1975). Global cooling may have reduced the amount of water vapor held in the atmosphere and thus produced additional cooling resulted from the greenhouse effect (Ruddiman, 2002). On the other hand, global cooling during the late Middle Miocene may have caused the replacement of forest by single-story vegetation types (Mudie and Helgason, 1983; Wolfe, 1980) in middle-high latitudes, thereby increasing albebo and inducing additional cooling (Dutton and Barron, 1997). Therefore, a more significant cooling may have occurred about 11 Ma ago, thereby aggravating the aridification in Central Asia.

6 CONCLUSION

The $\delta^{13}C$ and $\delta^{18}O$ records derived from the lacustrine-fluvial sediment sequence in Tianshui Basin reveal significant climate changes during the Miocene. Prior to 13.6 Ma, the average of $\delta^{18}O$ values is the most negative, indicating a very wet climate. We ascribe this wet climate condition to the well-known Middle Miocene Climate Optimum. From 13.6 to 11.0 Ma, the $\delta^{18}O$ values experienced a positive excursion, indicating a decrease in precipitation probably in response to the expansion of the East Antarctic Ice Sheet and global cooling since about 14 Ma. Since 11.0 Ma, the $\delta^{18}O$ values exhibited an abrupt positive shift toward the most positive values, indicating a persistent dry condition. We attribute this climatic change to the sustained global cooling, which may have reduced the amount of water vapor held in the atmosphere, thereby leading to further restrain of moist source to Central Asia and a permanent drying in Asian interior.

ACKNOWELDGMENTS

This work was support by the National Natural Science Foundation of China (Nos. 40721061, 40871098, 41023006, and 41072258), the National Basic Research Program of China (No. 2010CB833405) and the Open Foundation of State Key Laboratory Loess and Quaternary Geology, Institute of Earth Environment, CAS (No. SKLLQG1219). We are grateful to the two anonymous reviewers and editor G Yao for their insightful comments that have substantially improved the manuscript. We also thank T J Peng, B Liu, and S P Liu for assistance during field work. Our gratitude is also due to Prof. S Y Yu for useful comments and English improvement.

REFERENCES CITED

Alonso-Zarza, A. M., Zhao, Z., Song, C. H., et al., 2009. Mud-Flat/Distal Fan and Shallow Lake Sedimentation (Upper Vallesian–Turolian) in the Tianshui Basin, Central China: Evidence Against the Late Miocene Eolian Loess. *Sedimentary Geology*, 22: 42–51

An, Z. S., Kutzbach, J. E., Prell, W. L., et al., 2001. Evolution of Asian Monsoons and Phased Uplift of the Himalaya-Tibetan Plateau since Late Miocene Times. *Nature* 411: 62–66

Barron, E. J., 1985. Explanation of the Tertiary Global Cooling Trend. *Palaeogeography*, *Palaeoclimatology*, *Palaeoecology*, 50: 45–61

Cheng, X. R., Zhao, Q. H., Wang, J. L., et al., 2004. Data Report: Stable Isotopes from Sites 1147 and 1148. In: Prell, W. L., Wang, P., Blum, P., et al., eds., *Proceedings of the Ocean Drilling Program*: *Scientific Results*, 184: 1–12

Chung, C. H., Koh, Y. K., 2005. Palynostratigraphic and Palaeoclimatic Investigations on the Miocene Deposits in the Pohang Area, South Korea. *Review of Palaeobotany and Palynology*, 135: 1–11

Clift, P., Lee, J. I., Clark, M. K., et al., 2002. Erosional Response of South China to Arc Rifting and Monsoonal Strengthening: A Record from the South China Sea. *Marine Geology*, 184: 207–226

Cyr, A. J., Currie, B. S., Rowley, D. B., 2005. Geochemical Evaluation of Fenghuoshan Group Lacustrine Carbonates, North-Central Tibet: Implications for the Paleoaltimetry of the Eocene Tibetan Plateau. *The Journal of Geology*, 113: 517–533

Dettman, D. L., Kohn, M. J., Quade, J., et al., 2001. Seasonal Stable Isotope Evidence for a Strong Asian Monsoon throughout the Past 10.7 m.y.. *Geology*, 29(1): 31–34

Dettman, D. L., Fang, X. M., Garzione, C. N., et al., 2003. Uplift Driven Climate Change at 12 Ma: A Long $\delta^{18}O$ Record from the NE Margin of the Tibetan Plateau. *Earth and Planetary Science Letters*, 214: 267–277

Dutton, J. F., Barron, E. J., 1997. Miocene to Present Vegetation Changes: A Possible Piece of the Cenozoic Cooling Puzzle. *Geology*, 25(1): 39–41

Fan, M., Dettman, D. L., Song, C. H., et al., 2007. Climatic Variation in the Linxia Basin, NE Plateau, from 13.1 to 4.3 Ma: The Stable Isotope Record. *Palaeogeography*, *Palaeoclimatology*, *Palaeoecology*, 247: 313–328

Fang, X. M., Garzione, C., Voo, R. V. D., et al., 2003. Flexural Subsidence by 29 Ma on the NE Edge of Tibet from the Magnetostratigraphy of Linxia Basin, China. *Earth and Planetary Science Letters*, 210: 545–560

Flower, B. P., 1993. Middle Miocene Ocean-Climate Transition: High-Resolution Oxygen and Carbon Isotopic Records from Deep Sea Drilling Project Site 588A, Southwest Pacific. *Paleoceanography*, 8: 811–843

Flower, B. P., Kennett, J. P., 1994. The Middle Miocene Climatic Transition: East Antarctic Ice Sheet Development, Deep Ocean Circulation and Global Carbon Cycling. *Palaeogeography*, *Palaeoclimatology*, *Palaeoecology*, 108: 537–555

Goldsmith, J. R., Graf, D. L., Joensuu, O. I., 1955. The Occurrence of Magnesian Calcites in Nature. *Geochimica et Cosmochimica Acta*, 7: 212–230

Goldsmith, J. R., Graf, D. L., Heard, H. C., 1961. Lattice Constants of the Calcium-Magnesium Carbonates. *The American Minerilogist*, 46: 453–457

Guo, Z. T., Ruddiman, W. F., Hao, Q. Z., et al., 2002. Onset of Asian Desertication by 22 Myr Ago Inferred from Loess Deposits in China. *Nature*, 416: 159–163

Guo, Z. T., Peng, S. Z., Hao, Q. Z., 2004. Late Miocene-Pleicene Development of Asian Aridication as Recorded in the Red-Earth Formation in Northern China. *Global and Planetary Change*, 41: 135–145

Holbourn, A., Kuhnt, W., Schulz, M., et al., 2005. Impacts of Orbital Forcing and Atmospheric Carbon Dioxide on Miocene Ice-Sheet Expansion. *Nature*, 438: 483–487

Hough, B. G., Garzione, C. N., Wang, Z., et al., 2011. Stable Isotope Evidence for Topographic Growth and Basin Segmentation: Implications for the Evolution of the NE Tibetan Plateau. *Geological Society of America Bulletin*, 123: 168–185

Hui, Z. C., Li, J. J., Xu, H., et al., 2011. Miocene Vegetation and Climatic Changes Reconstructed from a Sporopollen Record of the Tianshui Basin, NE Tibetan Plateau. *Palaogeography*, *Palaeoclimatology*, *Palaeoecology*, 308: 373–382

Itoigawa, J., Yamanoi, T., 1990. Climatic Optimum in the Mid-Neogene of the Japanese Islands. In: Tsuchi, R., ed.,

Pacific Neogene Events, Their Timing, Nature and Inter-Relationship. University of Tokyo Press, Tokyo. 3–14

Jiang, H. C., Ding, Z. L., Xiong, S. F., 2007. Magnetostratigraphy of the Neogene Sikouzi Section at Guyuan, Ningxia, China. *Paleogeography*, *Palaeoclimatology*, *Palaeoecology*, 243: 223–234

Jiang, H. C., Ding, Z. L., 2008. A 20 Ma Pollen Record of East-Asian Summer Monsoon Evolution from Guyuan Ningxia, China. *Palaeogeography*, *Palaeoclimatology*, *Palaeoecology*, 265: 30–38

Jiang, H. C., Ji, J. L., Gao, L., et al., 2008. Cooling-Driven Climate Change at 12–11 Ma: Multiproxy Recoords from a Long Fluviolacustrine Sequence at Guyuan, Ningxia, China. *Palaeogeography*, *Palaeoclimatology*, *Palaeoecology*, 265: 148–158

Jiang, H. C., Ding, Z. L., 2010. Eolian Grain-Size Signature of the Sikouzi Lacustrine Sediments (C-Hinese Loess Plateau): Implications for Neogene Evolution of the East Asian Winter Monsoon. *Geological Society of America*, 122: 843–854

John, C. M., Karner, G. D., Mutti, M., 2004. $\delta^{18}O$ and Marion Plateau Backstripping: Combining Two Approaches to Constrain Late Middle Miocene Eustatic Amplitude. *Geology*, 32: 829–832

Kent-Corson, M., Ritts, B., Zhuang, G., et al., 2009. Stable Isotopic Constraints on the Tectonic, Topographic, and Climatic Evolution of the Northern Margin of the Tibetan Plateau. *Earth Planetary Science Letters*, 282: 158–166

Kim, S., O'Neil, J. R., 1997. Equilibrium and Nonequilibrium Oxygen Isotope Effects in Synthetic Carbonates. *Geochimica et Cosmochimica Acta*, 61: 3461–3475

Lear, C. H., Elderfield, H., Wilson, P. A., 2000. Cenozoic Deep-Sea Temperatures and Glocal Ice Volumes from Mg/Ca in Benthic Foraminiferal Calcite. *Science*, 287: 269–272

Leng, M. J., Marshall, J. D., 2004. Palaeoclimate Interpretation of Stable Isotope Data from Lake Sediment Archives. *Quaternary Science Reviews*, 6(23): 811–831

Li, G. J., Pettke, T., Chen, J., 2011. Increasing Nd isotopic Ratio of Asian Dust Indicates Progressive Uplift of the North Tibetan Plateau since the Middle Miocene. *Geology*, 39: 199–202

Li, G. J., Chen, J., Yang, C., 2013. Primary and Secondary Carbonate in Chinese Loess Discriminated by Trace Element Composition. *Geochimica et Cosmochimica Acta*, 103: 26–35

Li, H. C., Ku, T. L., 1997. $\delta^{13}C$-$\delta^{18}C$ Covariance as a Paleohydrological Indicator for Closed Basin Lakes. *Palaeogeography*, *Palaeoclimatology*, *Palaeoecology*, 133: 69–80

Li, J. J., Zhang, J., Song, C. H., et al., 2006. Miocene Bahean Stratigraphy in the Longzhong Basin, Northern Central China and Its Implicatiions in Environmental Change. *Science in China Series D: Earth Sciences*, 49: 1270–1279

Li, J. J., Fang, X. M., Vander Voo, R., et al., 1997. Late Cenozoic Magnetostratigraphy (11–0 Ma) of the Dongshanding and Wangjiashan Sections in the Longzhong Basin, Western China. *Geologe & Mijnbouw*, 76: 121–134

Lu, H., Wang, X., Li, L., 2010. Aeolian Sediment Evidence that Global Cooling has Driven Late Cenozoic Stepwise Aridification in Asia. *Geological Society*, *London*, *Special Pubications*, 342: 29–44

Pascual, R., Janreguizar, E. O., 1990. Evolving Climates and Mammal Faunas in Cenozic South America. *Journal of Human Evolution*, 19: 23–60

Ma, Y. Z., Li, J. J., Fang, X. M., et al., 1998. Pollen Assemblage in 30.6–5.0 Ma Redbeds of Linxia Regionand Climate Evolution. *Chinese Science Bulletin*, 43: 301–304 (in Chinese)

Miao, Y. F., Fang, X. M., Herrmann, M., et al., 2011. Miocene Pollen Record of KC-1 Core in the Qaidam Basin, NE Tibetan Plateau and Implications for Evolution of the East Asian Monsoon. *Palaeography*, *Palaeoclimatology*, *Palaeoecology*, 299: 30–38

Miller, K. G., Faribanks, R. G., Mountain, G. S., 1987. Tertiary Oxygen Isotope Synthesis, Sea Level History, and Continental Margin Erosion. *Paleoceanography*, 2: 1–19

Miller, K. G., Wright, J. D., Fairbanks, R. G., 1991. Unlocking the Icehouse: Oligocene–Miocene Oxygen Isotopes, Eustasy and Margin Erosion. *Journal of Geophysical Reseach*, 96: 6829–6848

Miller, K. G., Mountain, G. S., The Leg 150 Shipboard Party, Members of the New Jersey Coastal Plain Drilling Project, 1996. Drilling and Dating New Jersey Oligocene–Miocene Sequences: Ice Volume, Global Sea Level, and Exxon Records. *Science*, 271: 1092–1095

Mudie, P. J., Helgason, J., 1983. Palynological Evidence for Miocene Climatic Cooling in Eastern Iceland about 9.8 Myr Ago. *Nature*, 303: 689–692

Ramsein, G., Fluteau, F., Besse, J., et al., 1997. Effect of Orogeny: Plate Motion and Land-Sea Distribution on Eurasian Climate Change over the Past 30 Million Years. *Nature*, 386: 788–795

Retallack, G. J., 1992. Middle Miocene Fossil Plants from Fort Ternan (Kenya) and Evolution of African Grasslands. *Paleobiology*, 18: 383–400

Robert, C., Sterin, R., Acquaviva, R., 1986. Cenozoic Evolution and Significance of Clay Associations in the New Zealand Region of the Southwest Pacific, Leg 90. In: Kunnett, J. P., von der Borch, C. C., eds., Init. Rep. DSDP Washington D. C.. 90: 1225–1238

Rozankski, K., Araguas-Araguas, L., Gonfiantini, R., 1993. Isotopic Patterns in Modern Global Precipitation, In: Swart, P., Mckenzie, J. A., Lohmann, K. C., et al., eds., Climate Change in Continental Isotopic Records. Geophys. Monogr. 78, Am. Geophys. Union, Washington D.C.. 1–36

Ruddiman, W. F., 2002. Earth's Climate: Past and Future. W. H. Freman and Company, New York. 1–465

Saito, T., Yamanoi, T., Morohoshi, F., et al., 1995. Discovery of Mangrove Plant Pollen from the "Shukunohora Sandstone facies" Keyo Formation, Mizunami Group (Miocene), Gifu Prefecture, Japan. *The Journal of the Geological Society of Japan*, 101(9): 747–749 (in Japanese)

Savin, S. M., Douglas, R. G., Stehli, F. G., 1975. Tertiary Marine Paleotemperatures. *Geological Society of America*, 86: 1499–1510

Shackleton, N. J., Kennett, J. P., 1975. Paleotemperature History of the Cenzoic and the Initiation of Antarctic Glaciation: Oxygen and Carbon Isotope Analyses in DSDP Sites 277, 279 and 281. *Initial Reports of the Deep Sea Drilling Project*, 29: 743–755

Singh, R. K., Gupta, A. K., 2005. Systematic Decline in Benthic Foraminiferal Species Diversity Linked to Productivity Increases over the Last 26 Ma in the Indian Ocean. *Journal of Foraminiferal Reseach*, 35(3): 219–227

Stein, R., Robert, C., 1986. Siliciclastic Sediments at Sites 588, 590 and 591: Neogene and Paleoggene Evolution in the Southwest Pacific and Australian Climate. In: Kennett, J. P., von der Borch. C. C. eds., *Initial Reports of the Deep Sea Drilling Project*, 90: 1437–1455

Talbot, M., 1990. A Review of the Palaeohydrological Interpretation of Carbon and Oxygen Isotopic Ratios in Primary Lacustrine Carbonates. *Chemistry Geology*, 80: 261–279

Wang, Y., Deng, T., 2005. A 25 m.y. Isotopic Record of Paleodiet and Environmental Change from Fossil Mammals and Paleosols from the NE Margin of the Tibetan Plateau. *Earth and Planetary Science Letters*, 236: 322–338

Wang, W. M., Saito, T., Nakagawa, T., 2001. Palynostratigraphy and Climatic Implications of Neogene Deposits in the Himi Area of Toyama Prefecture, Central Japan. *Review of Palaeobotany and Palynology*, 117: 281–295

Webb, S. D., 1997. A History of Savanna Vertebrates in the New World. Part I: North America. *Annual Review of Ecology Systematics*, 8: 355–380

Wei, G. J., Li, X. H., Liu, Y., et al., 2006. Geochemical Record of Chemical Weathering and Monsoon Climate Change since the Early Miocene in the South China Sea. *Paleoceanography*, 21: PA4214, doi:10.1029/2006PA001300

White, J. M., Ager, T. A., Adam, D. P., et al., 1997. An 18 Million Year Record of Vegetation and Climate Change in Northwestern Canada and Alaska: Tectonic and Global Climatic Correlates. *Palaeogeography*, *Palaeoclimatology*, *Palaeoecology*, 130: 293–306

Wolfe, J. A., 1980. Tertiary Climates and Floristic Relationships at High Latitudes in the Northern Hemisphere. *Palaeogeography*, *Palaeoclimatology*, *Palaeoecology*, 30: 313–323

Wolfe, J. A. 1985. Distribuion of Major Vegetational Types during the Tertiary. In: Sundquist, E. T., Broecker, W. S. eds., The Carbon Cycle and Atmospheric CO_2: Natural Variations Archean to Persent. Geophys. Monogr. 32. AGU, Washington D.C.. 357–375

Yang, P., Sun, Z. C., Li, D. M., et al., 2000. Ostracoda Extinction and Explosion Events of the Mesozoic–Cenozoic in Qaidam Basin, Northwest China. *Journal of Palaeogeograhy*, 2(3): 69–74 (In Chinese with English Abstract)

Zachos, J., Pagani, M., Sloan, L., et al., 2001. Trends, Rhythms, and Aberratios in Global Climate 65 Ma to Present. *Science*, 292: 686–693

Zachos, J. C., Gerald, R. D., Richard, E. Z., 2008. An Early Cenozoic Perspective on Greenhouse: Warming and Carbon-Cycle Dynamics. *Nature*, 451(17): 279–283

Zhai, R. J., 1959. On a Collection of Miocene Mammals from Eastern Gansu. *Pleovertebrata et Paleoanthropologia*, 1: 139–140 (in Chinese)

Zhang, J., Li, J. J., Song, C. H., et al., 2013. Paleomagnetic Ages of Miocene Fluvio-Lacustrine Sediments in the Tianshui Basin, Western China. *Journal of Asian Earth Sciences*, 62: 341–348

Zhuang, G. S., Hourigan, J. K., Koch, P. L., et al., 2011. Isotopic Constraints on Intensified Aridity in Central Asia around 12 Ma. *Earth and Planetary Science Letters*, 312: 152–163

Zou, H. B., McKeegan, K. D., Xu, X. S., et al., 2004. Fe-Al-rich Tridymite-Hercynite Xenoliths with Positive Cerium Anomalies: Preserved Lateritic Paleosols and Implications for Miocene Climate. *Chemical Geology*, 207: 101–116